JOURNAL OF GEOPHYSICAL RESEARCH, VOL. 93, NO. B11, PAGES 13,355–13,366, NOVEMBER 10, 1988

68.

Slab Decoupling in the Tonga Arc: The June 22, 1977, Earthquake

PAUL R. LUNDGREN [1] AND EMILE A. OKAL

Department of Geological Sciences, Northwestern University, Evanston, Illinois

The June 22, 1977, earthquake in the southern Tonga arc is a large normal faulting event with down-dip rupture propagation on a steeply dipping fault plane. We use a standard least squares inversion of *P* and *SH* waves for the source time function to determine a source consisting of two subevents located at depths of 40–55 and 105–125 km and a total time duration of 50 s. The ratios of the spectral amplitudes of the radial modes ${}_0S_0$, ${}_1S_0$ and ${}_2S_0$ independently require a centroid depth of at least 100 km at their lower frequencies. The body wave analysis suggests a moment of 1.04×10^{28}, and the ${}_0S_0$ spectral amplitude suggests a value of 1.8–2.0 $\times 10^{28}$ dyn cm. The emerging picture is that of a complete rupture of the sinking lithospheric slab, starting from 40 km depth and propagating down to 125 km. This indicates that the decoupling of the overriding lithosphere from the slab in this area of the Tonga arc takes place by gravitational pull.

1. INTRODUCTION

Large subduction zone earthquakes at shallow depths are usually thrusting events at the interface of the two converging plates. However, some of the largest events associated with convergent plate boundaries involve normal faulting and have been interpreted as representing breaking of the subducting slab from the suboceanic lithosphere under the gravitational pull exerted by the sinking lithosphere [*Kanamori*, 1971*a*; *Abe*, 1972*a*,*b*]. Typical examples are the Sanriku earthquake of 1933, the March 30, 1965, Aleutian event, the Peruvian shock of May 31, 1970, and the August 19, 1977, Indonesia earthquake, most of which occurred seaward of the trench. The latter involved the largest seismic moment release in the past 23 years; however, some controversy remains as to the vertical extent of its rupture. *Silver and Jordan* [1983] and *Spence* [1986] have constrained it to very shallow depths (15 and 28 km, respectively) and have interpreted it as an expression of the bending of the lithosphere, while *Given and Kanamori* [1980] determined a rupture extending to 60–90 km, implying a nearly complete breaking of the slab, and supporting the concept of decoupling of the two pieces of lithosphere. In a recent study, *Welc and Lay* [1987] described a different case of decoupling in the Banda arc actually taking place through a very large (3×10^{28} dyn cm) thrust earthquake, involving overriding of the Australian continental lithosphere over the detaching slab.

In this paper, we focus on the June 22, 1977, Tonga earthquake. This event, by far the largest earthquake in the Tonga arc in the past 25, and possibly 65 years, occurred arcward of the trench and had a normal faulting focal mechanism. Figure 1 shows the general location of the epicenter in the Tonga arc. In order to assess the regime of rupture of the slab, it is in particular crucial to identify which of the two nodal planes (subvertical or subhorizontal one) is the actual fault plane. We use body wave deconvolution of long-period seismograms to retrieve the time function of the source and to optimize the depths of individual subevents. These results indicate that rupture extended over 80 km vertically, a picture also supported by the study of radial mode spectral amplitudes and implying complete breaking of the subducting slab by gravitational pull along a steeply dipping fault plane.

[1]Now at Istituto Nazionale di Geofisica, Rome, Italy.

Paper number 7B6103
0148-0227/88/007B-6103$05.00

2. THE JUNE 22, 1977 TONGA EVENT

Location and Size

This earthquake took place at 22.9°S, 175.8°W, midway between the trench and the volcanic island arc. Its conventional magnitudes were given as $m_b = 6.8$ (PDE), 6.3 (ISC); 7.2 (station PPT, Tahiti); and $M_s = 7.2$ (PDE, Pasadena, Berkeley). Magnitudes read at PPT (Papeete, Tahiti) were $m_b = 7.2$; $M_s = 7.8$ [*Talandier and Okal*, 1979]. Published estimates of the moment M_0 of the event are (in units of 10^{28} dyn cm): 1.4 [*Dziewonski et al.*, 1987], 1.5 [*Talandier and Okal*, 1979], 1.7 [*Talandier et al.*, 1987], and 2.3 [*Silver and Jordan*, 1983]. This generally amounts to an M_s:M_0 deficiency suggestive of anomalous depth, a long source duration, or both. Indeed, Silver and Jordan assigned the event a characteristic source duration $\tau_c = 66$ s, making it a "slow" earthquake.

Depth

The depth of this event remains a somewhat controversial issue, which provides the motivation for the present study. Solutions based on first arrival times are the Preliminary Determination of Epicenters (PDE) determination ($h = 65$ km) and the International Seismological Centre (ISC) ($h = 69$ km). On the basis of the interpretation of a strong second arrival as *pP*, *Talandier and Okal* [1979] proposed $h = 49$ km. Thus it is most probable that the earthquake rupture initiated at a depth of 40–70 km, corresponding grossly with the ceiling of the subducting slab at this location. However, the identification of *pP* can be unreliable for an earthquake which, as we will see, exhibits a complex source time function. On the other hand, the aftershock zone is suggestive of extended vertical rupture [e.g., *Silver and Jordan*, 1983]. Similarly, the large number of high-order overtone modes generated by the event [*Masters and Gilbert*, 1981; *Fukao and Suda*, 1987] suggests that the earthquake's centroid must be significantly deeper than usual for events of this size. Also, it should be noticed that the

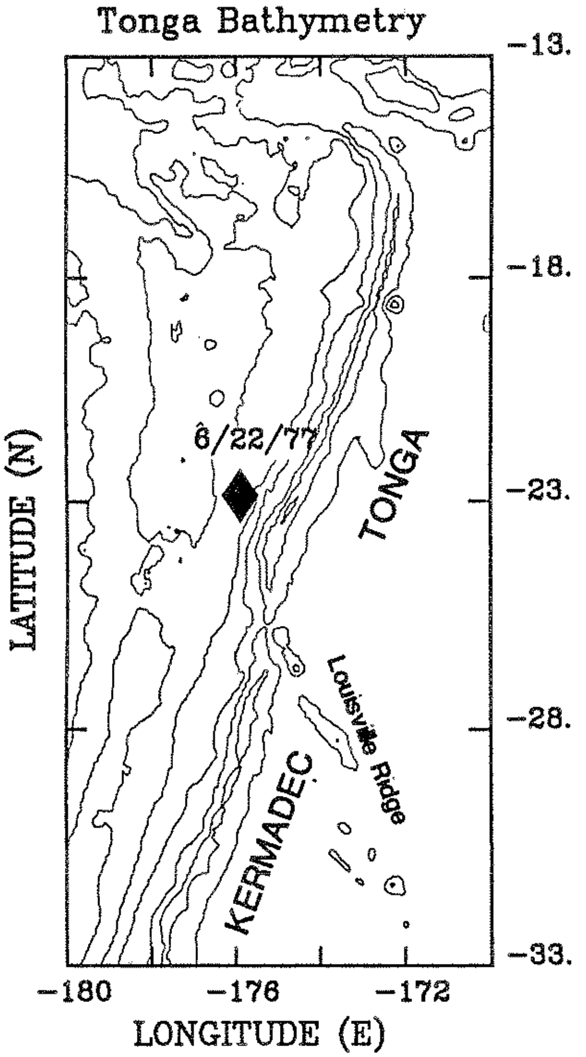

Fig. 1. Seismotectonic map of the Tonga arc. The large diamond is the epicenter of the June 22, 1977 event. Also featured is the Louisville Ridge.

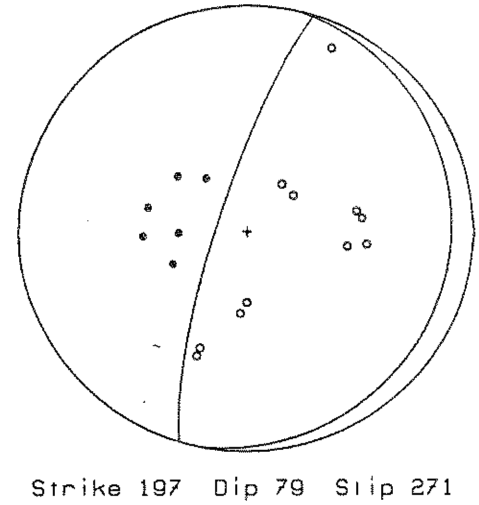

Fig. 2. Equal-area projection of the lower focal hemisphere of the June 22, 1977 Tonga main event. Solid circles represent compressional first motions; open circles represent dilatations, as read by the authors for this study. The fault planes traced are from the Harvard CMT solution.

ISC residuals at nearby stations are strongly positive and become negative at distances of 20°–40°. It is not clear whether this is due to lower than normal velocities in the backarc structures or to underestimation of depth as suggested by *Rees and Okal* [1987]. *Dziewonski et al.*'s [1987] centroid depth, obtained by moment tensor inversion, is 61.3 km, actually shallower than, but not significantly different from, the ISC first arrival depth; similarly, *Silver and Jordan* [1983] give a centroid depth of 65 km, which they "prefer" on the basis of the low-frequency spectrum of the moment release function, but their moment rate release curve versus frequency is less irregular at greater depths. On the other hand, *Giardini* [1984] commented that moment tensor solutions attempted from P waves alone led to a deeper centroid (130 km) and that a combination of P waves and surface waves resulted in much poorer fits. Finally, it should be emphasized that the moment of the earthquake and the depth to its centroid are clearly interdependent, as demonstrated, for example, by *Silver and Jordan* [1983].

This controversy strongly suggests that rupture propagated vertically during faulting. In this general framework, we use the technique of body wave deconvolution with variable source parameters to unravel the evolution of the source characteristics during the rupture. Also, we conduct an independent study of the excitation of the gravest radial modes of the Earth by the event to place further constraints on its centroid depth.

Focal mechanism

Two focal mechanism solutions are available for this event: G.S. Stewart and J.W. Given [personal communication, 1978] proposed strike $\phi = 200°$, dip $\delta = 73°$, slip $\lambda = 297°$. The Harvard centroid moment tensor (CMT) solution [*Dziewonski et al.*, 1987; *Giardini*, 1984] is $\phi = 197°$, $\delta = 79°$, $\lambda = 271°$.

Figure 2 shows P wave first motions, picked in this study, plotted with the CMT solution. Our first motion picks are in agreement with this mechanism. A steeply dipping nodal plane is well constrained by the data, but the slip angle along it could in principle vary from 235° to 280°. A cross section of aftershocks perpendicular to the nodal planes of the focal mechanism in Figure 3 shows a plane of seismicity dipping 75° to the west. This suggests that the steeply dipping nodal plane is indeed the plane of rupture.

3. BODY WAVE DECONVOLUTION

Method

In order to determine the complexity of the rupture and the distribution of moment release with depth we used the least squares body wave deconvolution method [*Ruff and Kanamori*, 1983], extended to conditions of evolving source characteristics as described in detail by *Wiens* [1985], *Stein and Wiens* [1986], and *Lundgren et al.* [1988], of which a brief summary follows.

Given a teleseismic body wave signal $s(t)$, which can be represented as the convolution $s(t) = m(t) * e(t) * i(t)$, we solve for the source time function $m(t)$. Grouping the

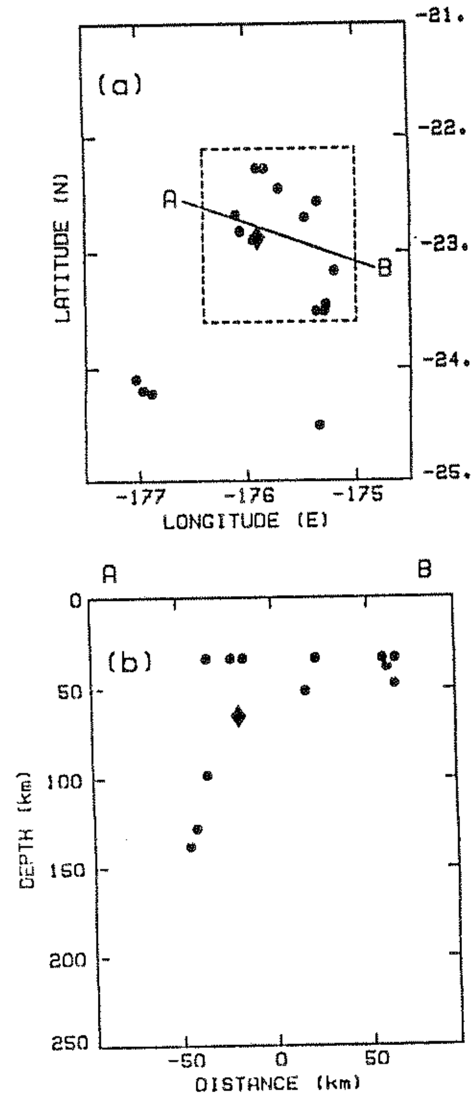

Fig. 3. One-week aftershock distribution of the June 22, 1977, earthquake. Diamond represents main event. In Figure 3a, aftershocks are in map view, with the area inclosed by the dashed line shown in Figure 3b as a cross section along line A-B, perpendicular to the strike of the fault plane.

impulse response of the Earth $e(t)$ and the instrument response $i(t)$ together, we write $s(t) = g(t) * m(t)$, where $g(t) = e(t) * i(t)$ is the Green's function for a particular mechanism and depth. The convolution, in vector-matrix form is $s_i = G_{ij} m_j$ where G is the Green's function matrix.

We use a damped Lanczos inversion to solve for the source time function **m** in the least-squares sense [*Lanczos*, 1961; *Ruff and Kanamori*, 1983]:

$$\mathbf{m} = \mathbf{G}' \mathbf{s} \tag{1}$$

with

$$\mathbf{G}' = (\mathbf{G}^T \mathbf{W} \mathbf{G} + d\, \mathbf{I})^{-1} \mathbf{G}^T \mathbf{W} \tag{2}$$

where $\mathbf{W} = \mathbf{I}(1/\mathrm{var}(\mathbf{s}))$ weights the inverted data set, d is the damping parameter, and I is the identity matrix. This formalism is not restricted to a single station and can simultaneously invert a multiple station dataset.

The application of the Lanczos inversion to complex body waves, which we will call the least squares method, is straightforward. At each step, the depth and fault geometry of an individual subevent in the source time function are chosen so as to minimize the squared error between residual data and synthetics. The synthetic seismogram for that subevent is then subtracted from the residual seismogram, and the process is iterated for the next subevent.

Application to the 1977 Tonga Event

We used *P* waves from the two Global Digital Seismograph Network (GDSN) stations ZOBO (La Paz) and CTAO (Charters Towers), and *SH* waves from the two GDSN stations NWAO (Perth) and CTAO. In these early stages of development of the GDSN network, we could not obtain a large good quality data set; also, because of the very large moment of the event, most *P* arrivals were off-scale on standard World-Wide Standard Seismograph Network (WWSSN) records. The seismic traces for the *P* waves were aligned with respect to each other by the apparent onset of the first motion. This alignment was maintained for all iterations. The alignment for the two *SH* traces used was done in the same way as the *P* waves but with the additional constraint of deconvolving the *SH* seismograms separately and aligning through small adjustments based on the timing of their source time functions.

P waves

We follow the procedure described in detail by *Lundgren et al.* [1988]. We first solve for the first pulse in the source by deconvolving *P* wave seismograms for the whole source time function at a range of depths. These results are presented on Figure 4, showing a minimum error at a depth of 60 km; however, because of the relatively flat well in the residual curve from 35 to 65 km, we investigated systematically the shape of synthetics built for first pulse depths of 25, 40, and 55 km. As shown on Figure 5, synthetics for the deeper source (55 km) gives too large an amplitude and a relatively poor fit to the first part of the waveforms. This is due to the fact that during this first iteration of the method, the program still attempts to fit the whole seismogram rather than the first part alone. In particular, if the amplitude of the source time function for the greater depth were scaled in order to match the amplitude of the first pulse, then the overall error at this greater depth would increase. For the lesser depths the fit to the initial waveform is achieved without any need for scaling the deconvolved source time function. On this basis, we prefer a depth of 40 km for the first pulse, as giving the best fit to the initial part of the seismogram. The solution for the 25-km depth is almost indistinguishable from the 40-km solution but is too shallow to be located in the subducting slab. We found that the 40-km depth was the depth nearest the error minimum which fit the initial waveform. The slip for the first pulse was determined to be 271° by deconvolving the seismograms at a range of slip values for a constant depth of 40 km. Figure 4*b* shows that this parameter is also poorly resolved by the data.

The depth and source time function of the second pulse were determined by deconvolving the residual data, formed by removing the contribution of the first pulse, over a range of

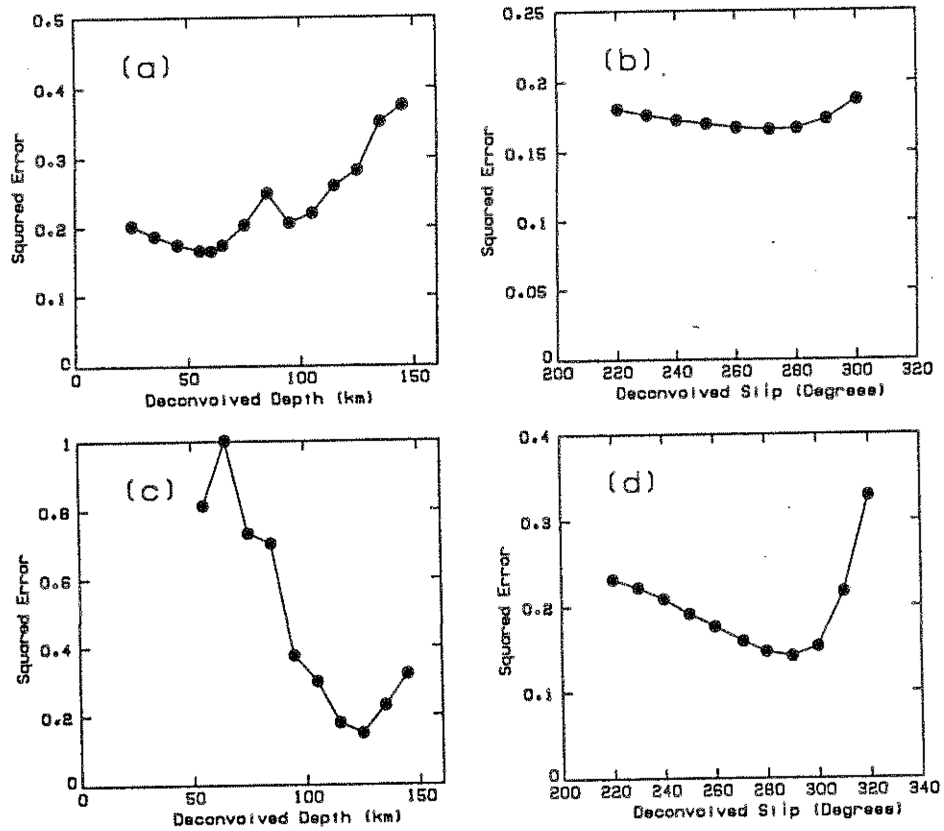

Fig. 4. Deconvolution of P waves. *(a)* Plots of least squares residuals as a function of depth of the first pulse. *(b)* Plots of least squares residuals as a function of slip angle for the first pulse, with depth constrained at 40 km. *(c)* Deconvolution of the residual seismogram data set: same as Figure 4*a* but for the second pulse. *(d)* Deconvolution of the residual seismogram data set: same as Figure 4*b* but for the second pulse.

depths, for a source time function windowed in time between 0 and 80 s. The time window was ended at 80 s to remove the effects of possible later spurious pulses. Figure 4*c* shows that the error minimum for the second pulse occurs at a depth of 125 km. The optimal slip vector at this depth is found to be 290° (Figure 4*d*).

The procedure was repeated for a possible third pulse. The results gave minima at the depths of the first two pulses and were very noisy. We do not regard a possible third pulse as clearly resolved or warranted by the data.

The combined results are shown in Figure 6. The source time function has a total duration of about 50 s and is composed of two pulses centered at 40 and 125 km. We computed seismic moments of 6.8×10^{27} and 3.6×10^{27} dyn cm for the first and second pulses, respectively, for a total moment of 10.4×10^{27} dyn cm. The centroid of these two pulses is at 69 km depth, which is the same as the ISC depth and slightly but not significantly deeper than the CMT solution for surface waves.

SH Waves

Figure 7*a* shows the results of deconvolving *SH* seismograms for NWAO and CTAO for depth. The minimum occurs at 55 km, as for P waves. The synthetics for the first pulse in the source time function are shown in Figure 8*a*. The fit to the first part of the waveforms does not require a depth shallower than 55 km for the first pulse, as in the case of P waves. The best slip was determined to be 250° by keeping the depth at 55 km and deconvolving for slip.

The synthetics for the first pulse were then subtracted from

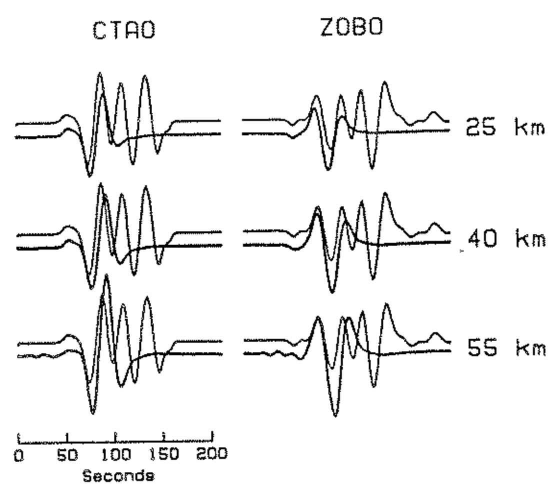

Fig. 5. Comparison of P wave data (thin line) and synthetics (thick line) computed from the first pulse in the source time function, for depths of 25–55 km. Synthetics are computed using a source time window of 0–60 s.

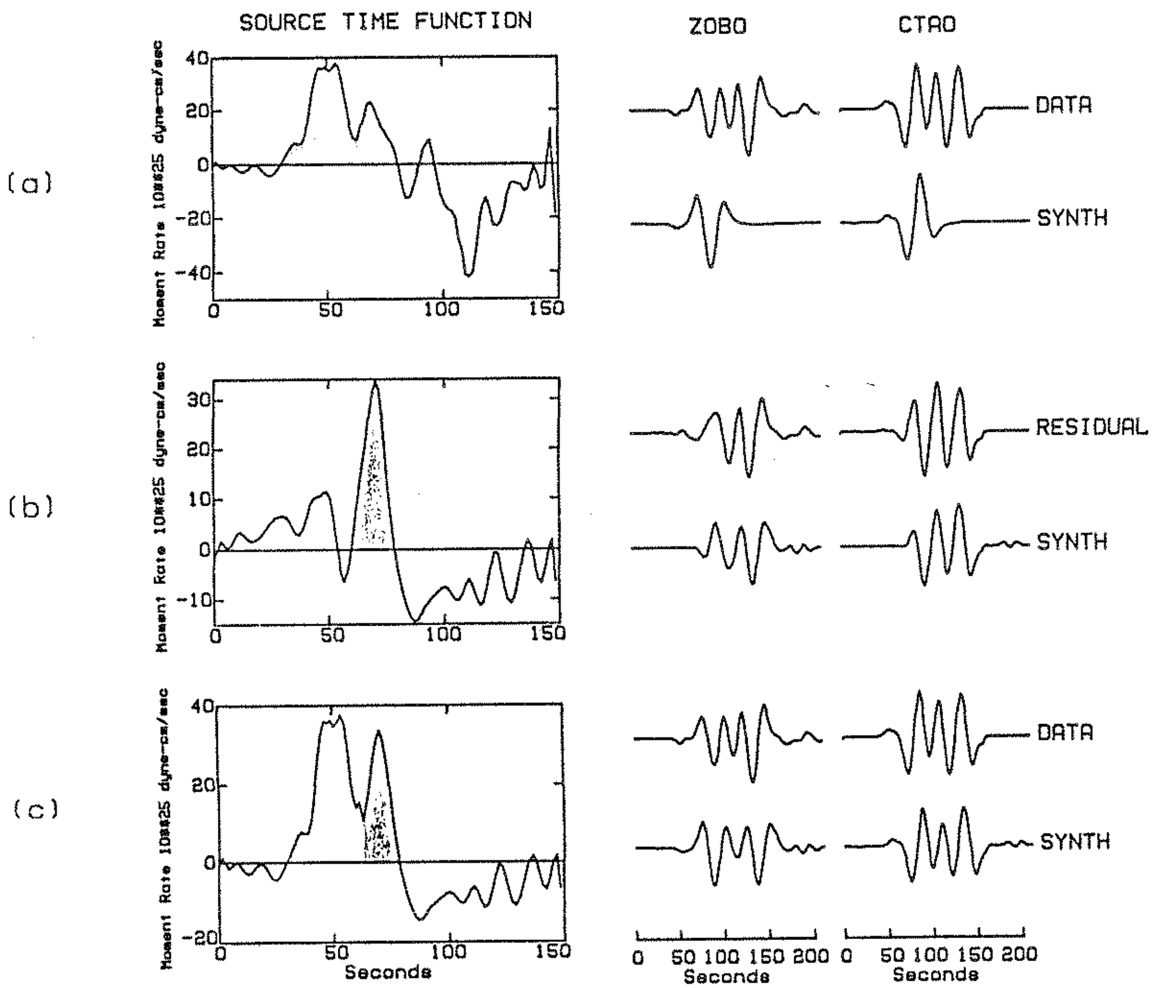

Fig. 6. Final source time function and comparison of P wave data and synthetics for stations CTAO and ZOBO. *(a)* Result of deconvolution of the first pulse. Only the stippled portion of the source is kept as the first pulse. *(b)* Result of the deconvolution of the residual (after subtraction from the data of the synthetic due to the first pulse as obtained in Figure 6*a*; only the dark portion is kept. *(c)* Final source combining Figures 6*a* and 6*b*.

the data and the procedure was repeated for the second pulse, using a time window of 0–80 seconds for the source time function. This is shown in Figure 7*c*. A depth of 105 km is determined for the second pulse. Figure 7*d* shows that a slip of 310° is preferred for the second pulse.

Both the P and SH wave results indicate downdip rupture with two main areas of moment release. The depths corresponding to the error minima for the first pulse for both datasets were in good agreement with each other and a lower value was retained only to achieve a better fit of the initial part of the P seismograms. In contrast, for the second pulse, the P waves preferred a depth 20 km greater than the SH waves. This difference may reflect lower depth resolution by SH waves, itself due to their lower-frequency content due to greater attenuation. While the optimal slip derived from the P waves agrees with the CMT solution for the first pulse and changes only 20° to a slip of 290° for the second pulse, the SH waves give a greater variation in slip values between the two pulses. The general character of dip-slip normal faulting is, however, unchanged. In conclusion, the emerging picture at this stage is that of a rupture initiating around 40 km, with the first source probably extending between 40 and 60 km. The second pulse, about half as intense as the first one, must be significantly deeper, in the vicinity of 125 km. There is no compelling evidence for a third pulse in the frequency range characteristic of the P and SH teleseismic body waves. Finally, there is some evidence for the development of a small component of strike-slip in the second pulse.

We have inverted the P and SH waves simultaneously and found that the inversions were dominated by the SH waves which have much larger absolute amplitudes than the P waves. Thus inverting both P and SH waves together gave the same results essentially as inverting the SH waves separately. Weighting down the S waves to alleviate this problem resulted in the loss of the moment amplitude information and did not alter the SH results substantially.

In an independent study, *Christensen and Lay* [this issue] have similarly used body wave deconvolution methods to extract the source characteristics of a number of earthquakes in the Tonga arc, including the June 22, 1977, event. These

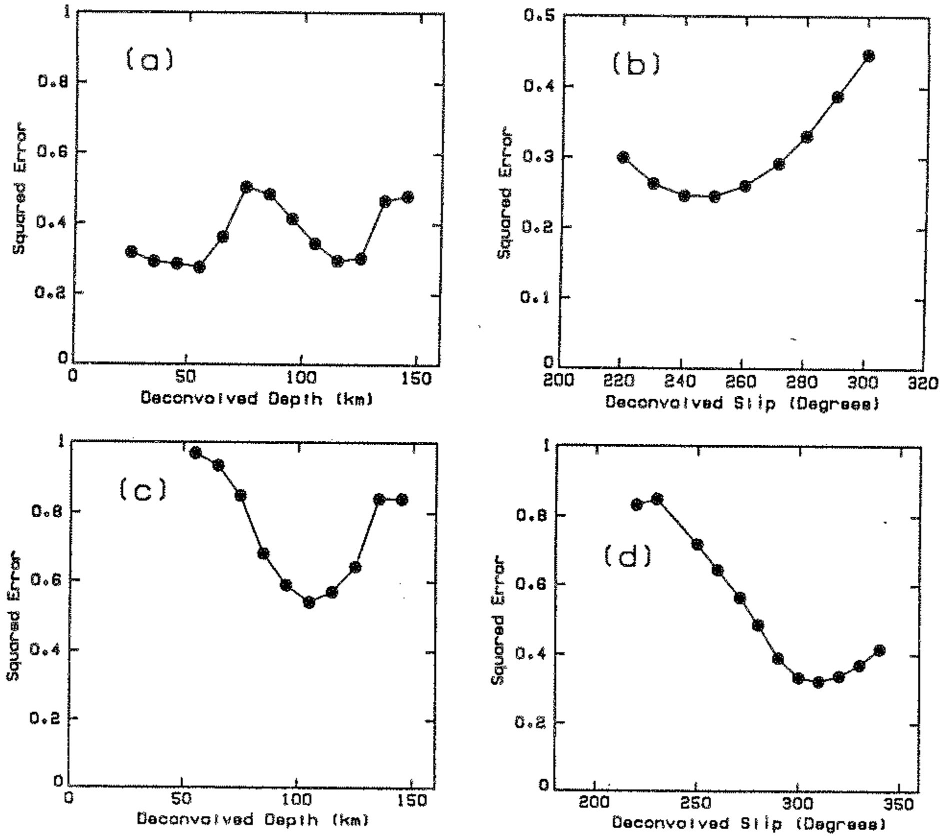

Fig. 7. Same as Figure 4 but for *SH* waves.

authors report that they were able to constrain the entire source of this event to depths no greater than 70 km. Since their results differ considerably from ours, it is necessary to discuss this discrepancy to some extent. *Christensen and Lay* [this issue] use a number of P wave deconvolution algorithms, mostly *Kikuchi and Kanamori*'s [1982] and *Kikuchi and Fukao*'s [1985]. While they prefer a source depth concentrated around 70 km, significant secondary minima of their normalized approximation error functions do develop for depths of 135–140 km, in good agreement with our preferred depth of 125 km for the second pulse. These secondary minima are robust, or even enhanced when the possible influence of any lateral heterogeneity in the source region on multistation inversion is taken into account. In this respect, the fact that *Christensen and Lay* [this issue] use a more complete set of stations does not seem compelling. We want to stress that our *SH* results confirm our interpretation based only on P waves; Christensen and Lay do not analyze S waves.

On the other hand, we note that in yet another recent body wave deconvolution study of the June 22, 1977, event, Ms. Sugi and T. Seno obtained results very similar to ours [T. Seno, personal communication, 1987]. At this point, it becomes increasingly probable that subtle differences between the two studies are probably responsible for their different results. In particular, differing weighting and damping schemes could affect the shape of the final normalized error versus depth curves.

In order to obtain more robust insight into the depth extent of the 1977 Tonga event, we conduct in section 4 a detailed study of its excitation of the three gravest Earth radial modes.

4. Excitation of Radial Modes

In this section we use spectral amplitudes of the Earth's radial modes excited by the 1977 Tonga earthquake to obtain independent estimates of the event's centroid at very low frequencies. Our purpose is to alleviate some of the possible trade-off between source geometry and depth inherent in moment tensor inversion [e.g., *Woodhouse*, 1981] by concentrating on the radial modes, whose excitation is relatively simple due to their high degree of symmetry. We are motivated in this study by the observation that ${}_1S_0$ is poorly, if at all, excited by the Tonga source (Figure 9).

Theory

Because a radial mode of the Earth ${}_nS_0$ involves neither horizontal displacements (y_3 in the notation of *Saito* [1967]) nor shear tractions (y_4), its excitation by a double-couple source is entirely controlled by only one coefficient (K_0 in the notation of *Kanamori and Cipar* [1974]), characteristic of a dipping fault plane, or in the moment tensor formalism of the combination $(M_{rr} - M_{\theta\theta} - M_{\phi\phi})$. In particular, the uniqueness of this coefficient means that the relative excitation of two radial modes ${}_nS_0$ and ${}_pS_0$ by a double-couple source is a function of depth only. Thus the ratio R_{np} of the spectral amplitudes of the two modes at a given station depends only on the depth of the source h_s, on the Q factors of the two

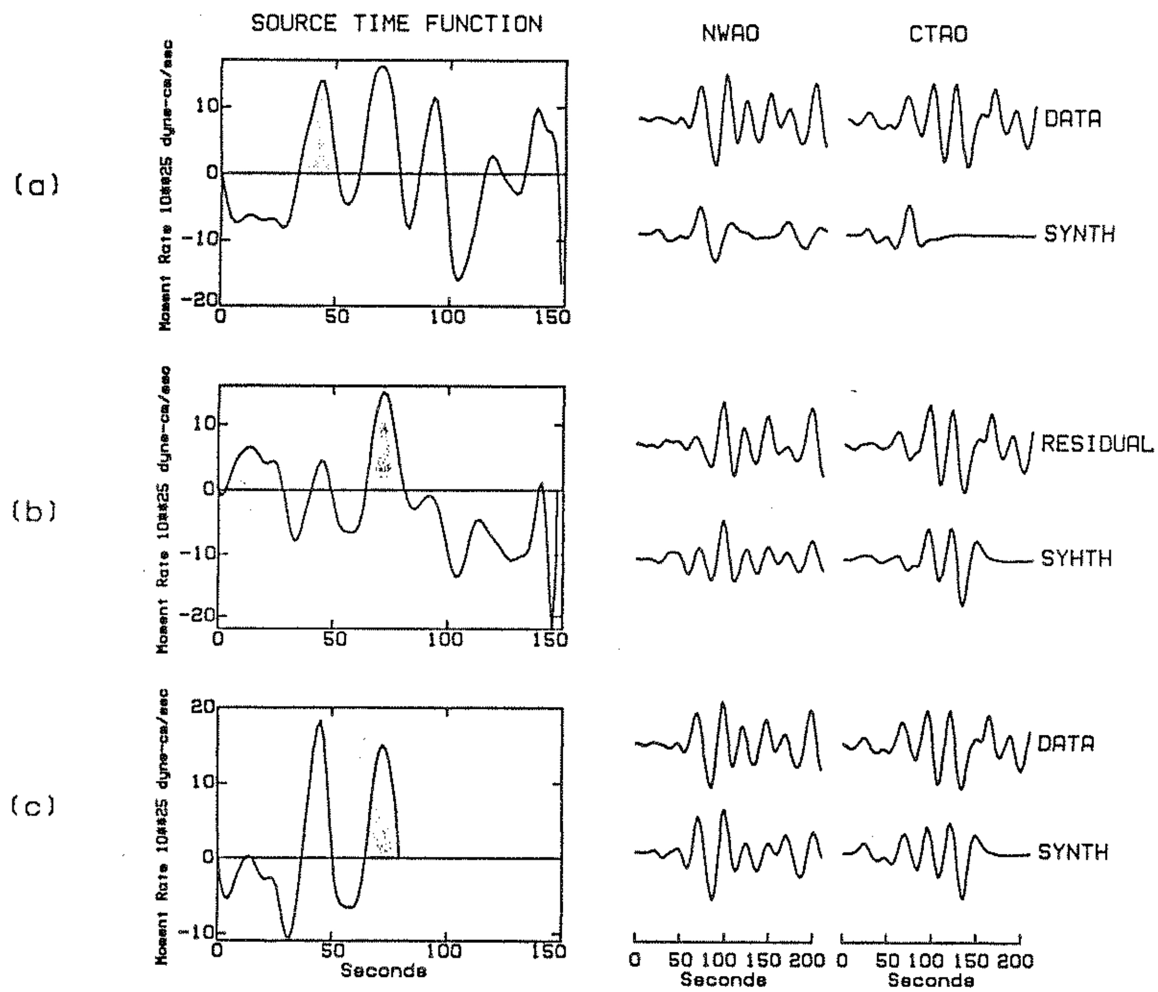

Fig. 8. Same as Figure 6 but for SH waves.

modes, and if the spectrum of the moment rate release function $\dot{M}(\omega)$ is not flat, on its relative values at the two angular eigenfrequencies ${}_n\omega_0$ and ${}_p\omega_0$. Specifically,

$$R_{n,p} = \left| \frac{{}_nK_0(h_s)}{{}_pK_0(h_s)} \frac{{}_nQF}{{}_pQF} \frac{\dot{M}({}_n\omega_0)}{\dot{M}({}_p\omega_0)} \right| \qquad (3)$$

where, for each mode, the attenuation quality factor is

$$QF = \frac{Q}{\omega}\left[\exp(-\omega t_i/2Q) - \exp(-\omega t_f/2Q)\right] \qquad (4)$$

and t_f and t_i are the final and initial times of the analyzed windows, measured after the origin time of the event.

In order to eliminate any possible uncertainty about the attenuation factors of the Earth's radial modes, we conduct two experiments for the 1977 Tonga and Indonesian (August 19) earthquakes using exactly identical time windows and stations in both cases. Specifically, we compare the ratios $R_{1,0}$ and $R_{2,0}$ of the spectral amplitudes of the three gravest radial modes in both cases [${}_0\omega_0 = (2\pi/1227)$ s^{-1}; ${}_1\omega_0 = (2\pi/607)$ s^{-1}; ${}_2\omega_0 = (2\pi/398)$ s^{-1}]. The introduction of this second earthquake adds, in principle, an additional unknown to the problem, namely, its hypocentral depth. The latter is in itself debated and controversial [*Given and Kanamori*, 1980; *Silver and Jordan*, 1983; *Spence*, 1986]. However, we will see that our data set resolves the Tonga depth practically independently of the Indonesia one; again, this approach eliminates the unknown Q factors in (4).

We use International Deployment of Accelerometers (IDA) data at the three stations BDF, SUR, and NNA. We eliminate other IDA stations, which did not provide records of comparably high quality for both events. We make use of windows of 655,360-s duration (approximately 1 week of data) starting 25.5 hours after the event in both cases. This rather late starting time helps clean out the signal from the fundamental Rayleigh modes and guards against nonlinearity in the instrument response, given the very large moment of the Indonesian shock. By using the same set of stations only 2 months apart in time, we also eliminate any uncertainty in the instrument responses. Finally, let us emphasize that the relative spectral amplitudes of the radial modes cannot be affected by horizontal directivity effects since these modes are are by definition insensitive to lateral displacement of the source.

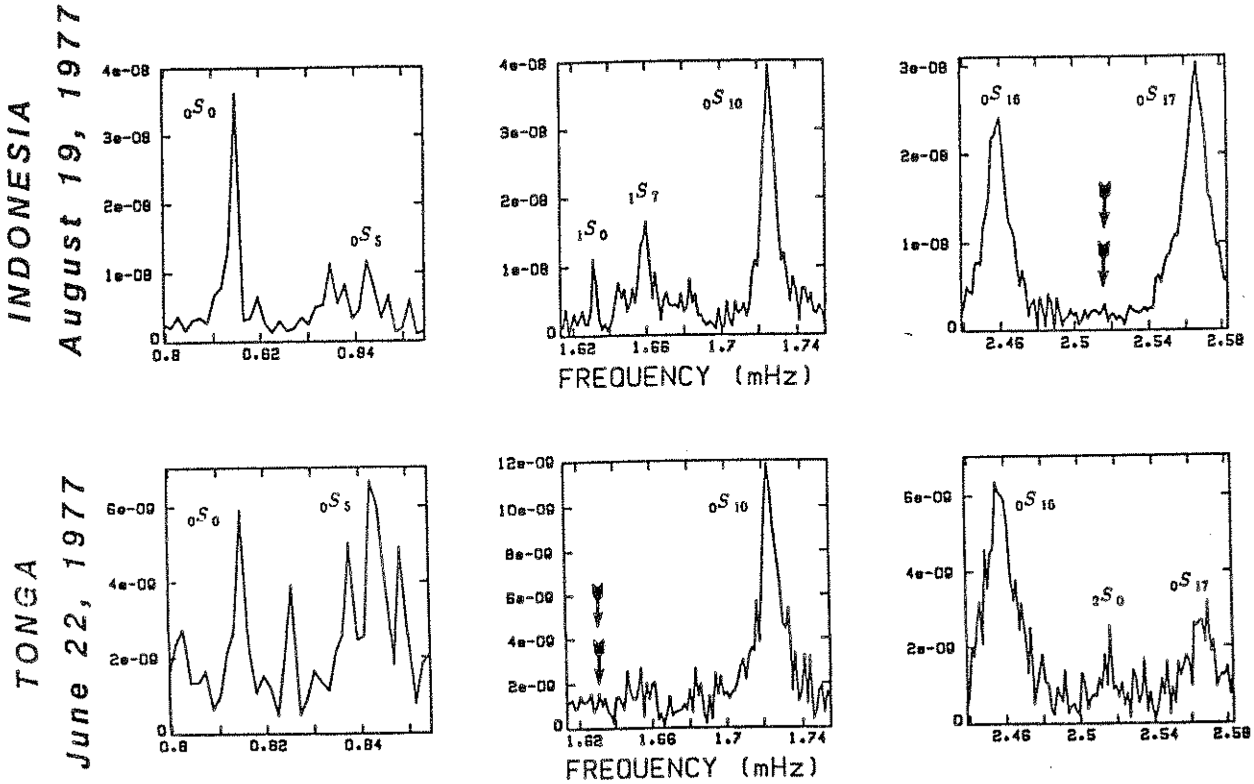

Fig. 9. Amplitude spectra at IDA station NNA in the vicinity of the frequencies of ${}_0S_0$, ${}_1S_0$, and ${}_2S_0$. (Top) August 19, 1977, Indonesia event. (Bottom) June 22, 1977, Tonga event. Vertical units are arbitrary but common to all six frames. Note absence of ${}_1S_0$ in the Tonga spectrum, and of ${}_2S_0$ in the Indonesia spectrum.

Results and Discussion

Figure 9 shows samples of spectra at NNA (Nanã, Peru), in the frequency ranges of ${}_0S_0$, ${}_1S_0$, and ${}_2S_0$. It is clear that ${}_1S_0$ is conspicuously absent from the spectra of the Tonga earthquake, while present for Indonesia; for ${}_2S_0$ the situation is reversed. Spectral stacking of the three stations reduces the noise and allows only tentative extraction of ${}_1S_0$ for the Tonga event, while it drastically enhances this mode for the Indonesian earthquake (Figure 10). It fails totally to extract ${}_2S_0$ for the Indonesian event. From this set of spectral amplitudes we can estimate "Tonga-to-Indonesia" ratios

$$ {}_{1,0}X_{T/I} = (R_{1,0})_{\text{Tonga}} \,/\, (R_{1,0})_{\text{Indonesia}} \leq 0.6 \qquad (5) $$

in the case of ${}_1S_0$, and

$$ {}_{2,0}X_{T/I} = (R_{2,0})_{\text{Tonga}} \,/\, (R_{2,0})_{\text{Indonesia}} \geq 1.3 \qquad (6) $$

in the case of ${}_2S_0$. The estimation of these constraints takes into account the level of noise in the spectrum and is in our opinion conservative.

In other words, there is deficiency of at least 40% in the excitation of ${}_1S_0$ relative to ${}_0S_0$ in the case of Tonga, as compared to Indonesia. According to equation (3), this can be controlled either by the influence of depth on the coefficients K_0, or by a strikingly deficient value of the moment rate release spectrum $\dot{M}$ around the frequency of ${}_1S_0$ in the case of the Tonga event.

The latter possibility deserves some discussion. *Silver and Jordan*'s [1983] analysis suggested a characteristic duration of 66 s, a figure in general agreement with our body wave investigation in section 3. For such τ_c, the deficiency of $\dot{M}({}_1\omega_0)$ with respect to $\dot{M}({}_0\omega_0)$ is only 2%; in order to produce a 40% deficiency, a source duration of at least 325 s is needed. Such an extremely slow source would be reflected in the fundamental modes at periods comparable to, or shorter than, 600 s. This is clearly not the case as evidenced from the spectrum of ${}_0S_{10}$ (Figure 9) and indeed from the results of *Silver and Jordan* [1983], whose study involved fundamental modes at precisely these periods. Furthermore, a very slow source for Tonga would tend to reduce the amplitude of ${}_2S_0$ even more than that of ${}_1S_0$, while the opposite is observed.

We therefore reject this explanation and contend that the deficiencies in excitation of ${}_1S_0$ for the Tonga event and of ${}_2S_0$ for the Indonesian event reflect the centroidal depths of the events. In Figure 11 we explore systematically the influence of the centroid depths of both events on the two ratios ${}_{1,0}X_{T/I}$ and ${}_{2,0}X_{T/I}$. As mentioned earlier, by using exclusively such ratios, we guard ourselves against possible uncertainties in the focal mechanisms and in the attenuation factors of the three modes. For each couple of depths we have used the PREM model [*Dziewonski and Anderson*, 1981] to compute theoretical values of the two ratios. These are con-

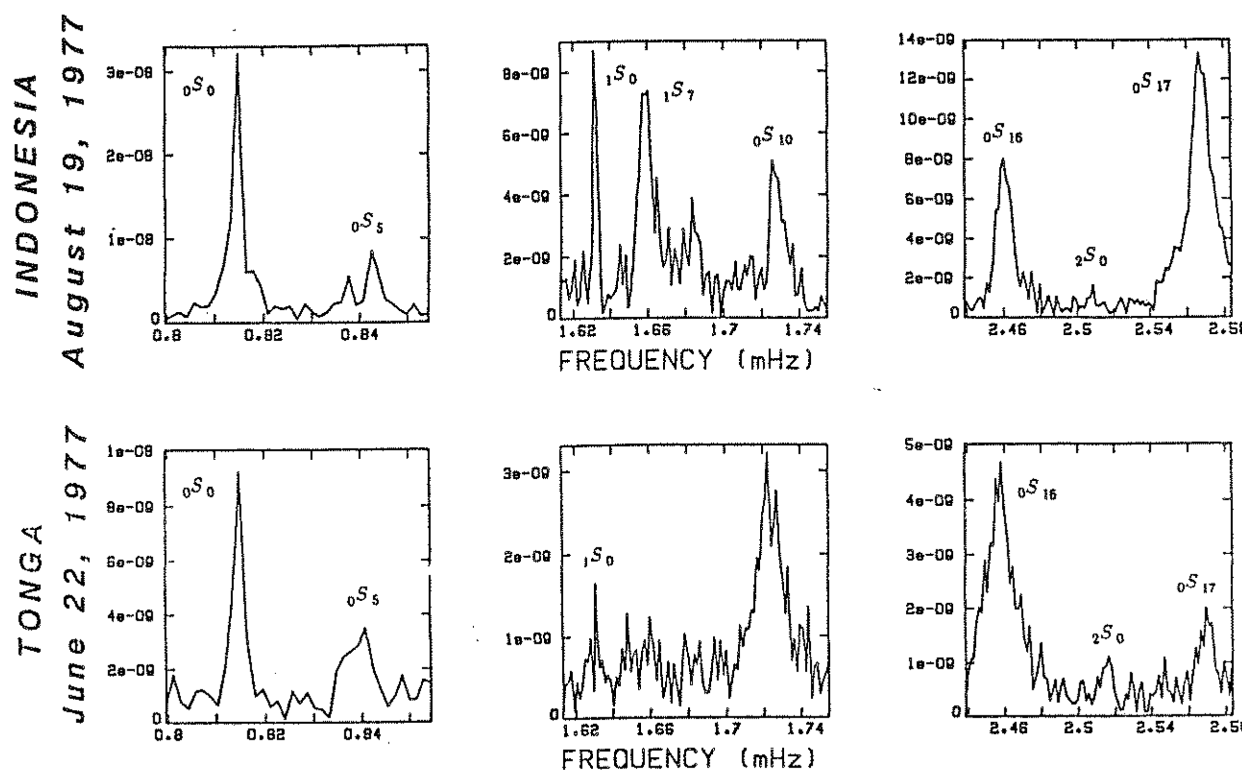

Fig. 10. Same as Figure 9, for stacked spectra of the three stations NNA, BDF, SUR. Note that this procedure extracts ${}_1S_0$ prominently for the Indonesian earthquake but only very tentatively for the Tonga event.

toured on the top two frames, with the areas violating the observational constraints (5) and (6) shaded. The remaining white area on Figure 11c is the locus of solutions satisfying both constraints. We let the Tonga depth vary between 40 and 220 km, and the Indonesia depth vary from 10 to 100 km. Both upper limits are clearly, but purposedly, excessive.

Tonga centroid depths comparable to the published CMT value (65 km) or to the results of our body wave deconvolution (69 km) violate the ${}_1S_0$ constraint for all Indonesia depths, predicting ${}_{1,0}X_{TI}$ ratios of the order of 0.8; furthermore, they also violate the ${}_2S_0$ constraint, by predicting a smaller excitation of ${}_2S_0$ by Tonga than by Indonesia, except if the Indonesian earthquake is placed at the node of excitation of the latter mode (around 70 km). This is an exceedingly deep and unlikely centroid for an event occurring seaward of the trench, in an area where the existence of brittle material at such depths would be hard to justify.

On the other hand, a Tonga centroid depth of 100 km satisfies both constraints for shallow values (say, less than 35 km) of the Indonesian centroid. This centroid would agree with *Giardini*'s [1984] suggested value of 130 km. The data set clearly has more resolution of the Tonga depth than of the Indonesian depth, and cannot be used to resolve the controversy about the latter's depth.

Thus, on the basis of the relative excitation of the Earth's radial modes, we require a centroid depth of at least 100 km for the June 22, 1977, Tonga event. In particular, when compared with the hypocenter of the first pulse, this centroid confirms vertical propagation of the rupture, and rules out the conjugate mechanism (rupture at a shallower depth on a quasi-horizontal fault plane). We propose to interpret this greater centroidal depth as due to a slow, long-period, extension to the second pulse evidenced by the body wave deconvolution (at a depth of 125 km). Because this source would be slow, it would not contribute significantly to the body waves. In order to bring the final centroid to 100 km, the moment of the second pulse needs to be about 1.6×10^{28} dyn cm, for a total zero-frequency moment of the order of 2.3×10^{28} dyn cm. This is significantly more than suggested by the published solutions [*Dziewonski et al.*, 1987; *Giardini*, 1984; *Talandier et al.*, 1987] but in excellent agreement with *Silver and Jordan*'s [1983] preferred value. If the slow source is allowed to propagate deeper than 125 km, the total moment is reduced correspondingly. Regarding Silver and Jordan's results, their "preferred" value of ths static moment is obtained at a depth of 65 km but would be similar for a centroidal depth of 100 km, with a somewhat longer characteristic time. Thus our model is in agreement with these authors' results.

Finally, an independent measurement of the zero-frequency moment can also be obtained from the comparison of the stacked spectral amplitudes of ${}_0S_0$ for the Indonesian and Tonga events

$$\frac{A({}_0S_0)_T}{A({}_0S_0)_I} = \frac{M_{0(T)}}{M_{0(I)}} \cdot \left| \frac{K_0\,(100\text{ km})}{K_0\,(25\text{ km})} \cdot \frac{s_{R\,(T)}}{s_{R\,(I)}} \right| \qquad (7)$$

(where subscripts T and I represent Tonga and Indonesia respectively), measured on Figure 10 to be 0.26 . For ${}_0S_0$ the excitation coefficient K_0 varies less than 10% between 10 and 120 km, so that the result will be robust with respect to uncer-

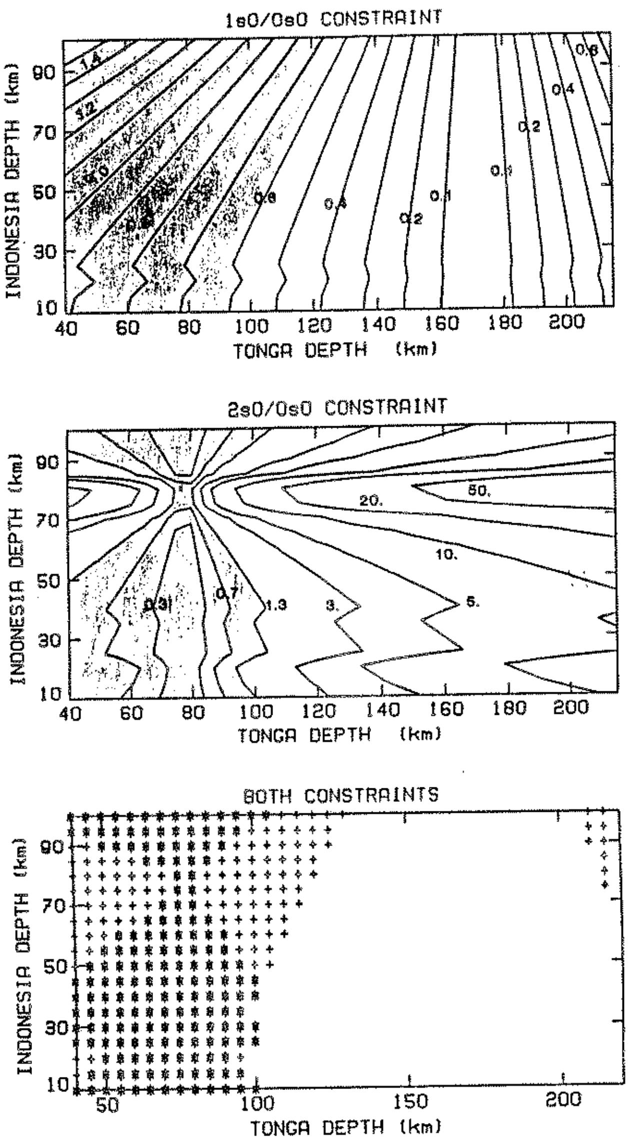

Fig. 11. Relative excitation of the three gravest radial modes by the Tonga and Indonesia events. In Figures 11*a* and 11*b*, we contour values of ${}_{1,0}X_{T/I}$ and ${}_{2,0}X_{T/I}$, respectively, and shade the areas violating the observed constraints. In Figure 11c we combine the two constraints: crosses correspond to solutions violating the ${}_1S_0$ constraint (equation (5)); asterisks indicate violation of the ${}_2S_0$ constraint (equation (6)). This diagram requires a minimal centroidal depth of 100 km for the Tonga event.

tainty in the centroid depths. We use the Harvard CMT solution for the Indonesian event ($\delta = 24°$; $\lambda = 287°$), yielding $s_{R\,(\mathrm{Indonesia})} = -0.36$, and the focal mechanism of the second pulse for the Tonga event ($s_{R\,(\mathrm{Tonga})} = -0.20$). This translates into a moment $M_{0\,(Tonga)}$ 0.49 times that of the Indonesian earthquake, or 1.8×10^{28} dyn cm using the Harvard value for $M_{0\,(\mathrm{Indonesia})}$ [*Dziewonski et al.*, 1987], or 2.0×10^{28} dyn cm using *Given and Kanamori*'s [1980] slightly larger estimate. A total moment of 2×10^{28} dyn cm would require a "slow" component of just under 10^{28} dyn cm at a depth of 134 km.

Finally, it should be noticed that the excitation, by the 1977 Tonga event of a substantial tsunami (10–15 cm Pacific-wide) cannot help discriminate between the two models preferred by ourselves and Sugi on one hand, and Christensen and Lay on the other: *Okal* [1988] has shown that depth is only a minor parameter in tsunami excitation: more specifically, for comparable values of the total moment, the amplitudes of tsunamis generated by the two sources differ by a factor of only 1.5 at a typical station such as PPT. Because of the difficulty of separating an absolute measurement of the high seas component of the tsunami from the effect of shoaling, as well as the uncertainty on the total moment, the tsunami amplitude information cannot be used to reject our model.

5. Discussion and Conclusions

As determined from the source functions of the body waves, the 100-km centroid of the radial modes, and the distribution of aftershocks, the source of the June 22, 1977, Tonga earthquake extended vertically over more than 80 km, suggesting complete rupture of the sinking lithospheric slab. The total moment obtained from body wave deconvolution is 1.0×10^{28} dyn cm, somewhat less than the 1.4–1.7 reported in the literature. However, in view of the "slow" character of the event reported by *Silver and Jordan* [1983], this discrepancy simply reflects the limited frequency spectrum of the body waves. Our radial mode study suggests a larger moment in the 1.8–2.0 $\times 10^{28}$ dyn cm range, in agreement with Silver and Jordan's estimate. The combination of moment and depth extent clearly makes this earthquake one of the largest intermediate depth events ever recorded, second only to the Banda Sea earthquake of 1963 [*Osada and Abe*, 1981; *Welc and Lay*, 1987].

In addition, both parts in our study can rule out interpreting the mechanism of the Tonga event as rupture on the conjugate, quasi-horizontal plane. It is clear that the mechanism of rupture of the lithospheric slab by thrust delamination along a gently dipping plane, as evidenced by *Welc and Lay* [1987] in the Banda Sea, results from the exceptional situation of buoyancy due to the presence of continental material on the Australian plate.

As shown on the tectonic cartoon (Figure 12), the 1977 Tonga event corresponds to the same decoupling process between the oceanic plate and the slab, as already recognized for the 1933 Sanriku, 1965 Aleutian, 1970 Peru, and 1977 Indonesian earthquakes [*Kanamori*, 1971*a*,*b*; *Abe*, 1971*a*,*b*; *Given and Kanamori*, 1980]. The small component of strike-slip developing in the later stage of the rupture is also shown on Figure 12. Its direction is in agreement with the expected

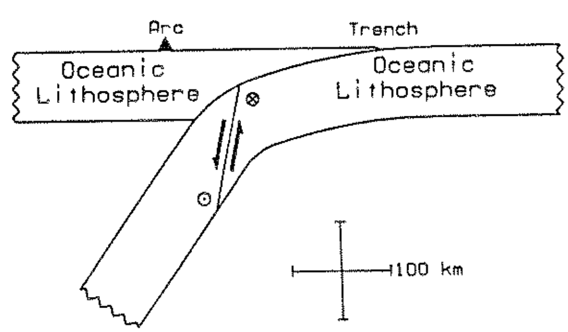

Fig. 12. Tectonic cartoon. Sense of motion on fault is indicated by arrows.

relative motion between a detached slab, sinking vertically (or at best along the line of steepest descent in the Benioff plane) under its own weight into the mantle, and the oceanic lithosphere, whose absolute motion in the area is oriented N59°W [*Minster and Jordan*, 1978], about 14° clockwise of the direction of dip of the slab.

However, significant differences do exist between the situations at the various subduction zones where large normal faulting events have been reported. Perhaps most strikingly, the Tonga event occurred 150 km arcward of the trench, as opposed to just above it or slightly oceanward as in the case of the Sanriku, Aleutian, and Indonesian earthquakes. The only similar case is that of the Peruvian earthquake; however, the latter, taking place in a strongly coupled subduction zone, with a low dip angle, did not extend to intermediate depth. The 1977 Tonga is also rather unique in that it is not in an obvious aftershock relationship with a large interplate thrust fault earthquake, as are clearly the Peru, Aleutian, and possibly Sanriku shocks. The only large earthquake having taken place in the area, prior to the 1977 event is the October 11, 1975, earthquake, which took place about 250 km to the SSE. However, *Christensen and Lay* [this issue] interpret its mechanism as intraplate, a conclusion upheld by its relatively low moment of only 1.4 to 1.9 $\times 10^{27}$ dyn cm [*Christensen and Lay*, this issue; J. Talandier, personal communication, 1987].

In this respect, the Tonga shock is closest to the Indonesia one, which occurred independently of a major thrusting event. This clearly illustrates the relatively decoupled nature of the Tonga subduction zone [*Uyeda and Kanamori*, 1979; *Uyeda*, 1987] and indicates that the rupture of the sinking slab in this region is an intraplate phenomenon, controlled by gravitational slab pull, rather than due to a rebound activated by the collision process.

Finally, we wish to discuss the location of the June 22, 1977, Tonga earthquake in relation to the subduction of the Louisville Ridge. This prominent feature of the South Pacific Basin floor, generally regarded as the trace of a hotspot in the prolongation of the Eltanin Fracture Zone, intersects the trench around 26°S and separates two regimes of subduction: to the north, the Tonga slab dips about 53°, while to the south, the Kermadec slab plunges a steeper 65°. As noted on a global scale by *Kelleher and McCann* [1976] and *Vogt et al.* [1976], the region at the trench-ridge intersection features a substantial deficiency in shallow, interplate seismicity (see Figure 1), although the few mechanisms available are in general compatible with thrust faulting at the trench. Holocene volcanism is also deficient between latitudes 20° and 26°S. Although the June 22, 1977, event occurred 300 km to the north of the Louisville ridge collision zone and because the latter's strike on the Pacific ocean is about N25°W, its trace on the descending slab is expected to lie in the immediate three-dimensional vicinity of the 1977 fault zone. In a potentially similar situation in Vanuatu, *Chung and Kanamori* [1978] have explained the occurrence of a moderately large ($M_0 = 5 \times 10^{26}$ dyn cm) intermediate depth earthquake as movement, predominantly of the strike-slip type, along a consumed passive tectonic feature, in that case the d'Entrecasteaux Ridge. In the case of Tonga, both the size of the 1977 event (30–40 times larger in terms of M_0) and its focal mechanism suggest to interpret it in terms of total decoupling of the descending slab, rather than reactivation of motion along the ridge. However, one can speculate that the generally buoyant character of the ridge [e.g., *Cazenave and Dominh*, 1984], which presumably inhibits the subduction, may contribute to the local accumulation of stress induced by the gravitational slab pull, and may be eventually responsible for the large size of the event.

Christensen and Lay [this issue] present a model in which the 1977 Tonga earthquake is the expression of the release of tensional stress accumulating locally under the strong coupling resulting from the collision of the buoyant Louisville Ridge with the trench. Their model must eventually predict very large thrust events, which will release the stress at this locked location. The moment of the 1982 event (about 10^{27} dyn cm) clearly does not qualify it as such. Apart from the June 22, 1977, event, the historical record provides only one truly large event in the region, on April 16, 1937. *Gutenberg and Richter* [1953] list it as $M = 8.1$, and the *Seismological Society of America* [1980] as $M = 7.9$; all listings show that it is deep, and we have relocated it at 310 km, using arrival times available from the International Seismological Summary. Thus we confirm that no truly large interplate subduction earthquakes are known in this portion of the Tonga arc, at least for the past 65 years. Therefore, and in conclusion, we prefer a model in which this portion of the subduction is decoupled; in that framework the 1977 earthquake can readily be interpreted as the rupturing of the whole slab under gravitational slab pull.

Acknowledgments. We thank Thorne Lay for a thorough review of the paper, Doug Christensen and Lay for good-spirited competition, and the participants in the Monday afternoon poster session at the 1987 San Francisco AGU for constructive discussions; especially Tetsuzo Seno, who mentioned to us the study by Ms. Sugi. Jacques Talandier provided seismic moments in advance of publication. Finally, we are grateful to the Editors of JGR, who coordinated the publication of the two studies side by side. This research was supported by the National Science Foundation under grant EAR-84-05040.

REFERENCES

Abe, K., Lithospheric normal faulting beneath the Aleutian Trench, *Phys. Earth Planet. Inter.*, *5*, 190–198, 1972*a*.

Abe, K., Mechanisms and tectonic implications of the 1966 and 1970 Peru earthquakes, *Phys. Earth Planet. Inter.*, *5*, 367–379, 1972*b*.

Cazenave, A., and K. Dominh, Geoid heights over the Louisville Ridge (South Pacific), *J. Geophys. Res.*, *89*, 11,171–11,179, 1984.

Christensen, D.H., and T. Lay, Large earthquakes in the Tonga region associated with the subduction of the Louisville Ridge, *J. Geophys. Res.*, this issue.

Chung, W.-Y., and H. Kanamori, Subduction process of a fracture zone and aseismic ridges — The focal mechanism and source characteristics of the New Hebrides earthquake of 1969 January 19 and some related events, *Geophys. J. R. Astron. Soc.*, *54*, 221–240, 1978.

Dziewonski, A.M., and D.L. Anderson, Preliminary reference Earth model, *Phys. Earth Planet. Inter.*, *25*, 297–356, 1981.

Dziewonski, A.M., G. Ekström, J.E. Franzen, and J.H. Woodhouse, Global seismicity of 1977; Centroid-moment tensor solutions for 471 earthquakes, *Phys. Earth Planet. Inter.*, *45*, 1–36, 1987.

Fukao, Y., and N. Suda, Detection of core modes from the Earth's free oscillation and structure of the inner core, paper presented at XIXth General Assembly, Int. Union of Geod. and Geophys., Vancouver, B.C., 1987.

Giardini, D., Systematic analysis of deep seismicity: 200 centroid-moment tensor solutions for earthquakes between 1977 and 1980, *Geophys. J. R. Astron. Soc.*, *77*, 883–914, 1984.

Given, J.W., and H. Kanamori, The depth extent of the 1977 Sumbawa, Indonesia earthquake (abstract), *Eos Trans. AGU*, *61*, 1044, 1980.

Gutenberg, B., and C.F. Richter, *Seismicity of the Earth and Associated Phenomena*, 310 pp., Princeton University Press, Princeton, N. J., 1953.

Kanamori, H., Seismological evidence for lithospheric normal faulting—The Sanriku earthquake of 1933, *Phys. Earth Planet. Inter.*, *4*, 289–300, 1971*a*.

Kanamori, H., Great earthquakes at island arcs and the lithosphere, *Tectonophysics, 12*, 187–198, 1971*b*.

Kanamori, H., Seismic and aseismic slip along subduction zones and their tectonic implications, in *Island Arcs, Deep-sea Trenches and Back-arc Basins, Maurice Ewing Ser.*, vol. 1, edited by M. Talwani and W. C. Pitman III, pp. 163–174, AGU, Washington, D. C., 1977.

Kanamori, H., and J.J. Cipar, Focal process of the great Chilean earthquake, May 22, 1960, *Phys. Earth Planet. Inter., 9*, 128–136, 1974.

Kelleher, J., and W.R. McCann, Buoyant zones, great earthquakes and unstable boundaries of subduction, *J. Geophys. Res., 81*, 4885–4896, 1976.

Lanczos, C., *Linear Differential Operators*, Van Nostrand, London, 1961.

Lundgren, P.R., E.A. Okal and S. Stein, Body wave deconvolution for variable source parameters; application to the December 6, 1978 Kuriles earthquake, *Geophys. J. R. Astron. Soc.*, in press, 1988.

Masters, T.G., and J.F. Gilbert, Structure of the inner core inferred from observations of its spheroidal shear modes, *Geophys. Res. Lett., 8*, 569–571, 1981.

Minster, J.-B., and T.H. Jordan, Present-day plate motions, *J. Geophys. Res., 83*, 5331–5354, 1978.

Okal, E.A., Seismic parameters controlling far-field tsunami amplitudes: A review, *Nat. Hazards J., 1*, 67-96, 1988.

Osada, M., and K. Abe, Mechanism and tectonic implications of the great Banda Sea earthquake of November 4, 1963, *Phys. Earth Planet. Inter., 25*, 129–139, 1981.

Rees, B.A., and E.A. Okal, The depth of the deepest historical earthquakes, *Pure Appl. Geophys., 125*, 699–715, 1987.

Ruff, L.J., and H. Kanamori, The rupture process and asperity distribution of three great earthquakes from long-period diffracted *P* waves, *Phys. Earth Planet. Inter., 31*, 202–230, 1983.

Saito, M., Excitation of free oscillations and surface waves by a point source in a vertically heterogeneous Earth, *J. Geophys. Res., 72*, 3689–3699, 1967.

Seismological Society of America, *Seismology Microfiche Publications from the Caltech Archives, Ser. II and III*, edited by J.R. Goodstein, H. Kanamori and W.H.K. Lee, Berkeley, Calif., 1980.

Silver, P.G., and T.H. Jordan, Total-moment spectra of fourteen large earthquakes, *J. Geophys. Res., 88*, 3273–3293, 1983.

Spence, W., The 1977 Sumba earthquake series: Evidence for slab pull force acting at a subduction zone, *J. Geophys. Res., 91*, 7225–7239, 1986.

Stein, S., and D.A. Wiens, Depth determination for shallow teleseismic earthquakes: Methods and results, *Rev. Geophys., 24*, 806–832, 1986.

Talandier, J., and E.A. Okal, Human perception of *T* waves: The June 22, 1977 Tonga earthquake felt on Tahiti, *Bull. Seismol. Soc. Am., 69*, 1475–1486, 1979.

Talandier, J., D. Reymond and E.A. Okal, M_m: Use of a variable-period mantle magnitude for the rapid one-station estimation of teleseismic moments, *Geophys. Res. Lett., 14*, 840–843, 1987.

Uyeda, S., Chilean vs. Mariana type subduction zones with remarks on arc volcanism and collision tectonics, in *Circum-Pacific Orogenic Belts and Evolution of the Pacific Ocean Basin, Geodyn. Ser.*, vol. 18, edited by J.W.H. Monger and J. Francheteau, pp. 1–7, AGU, Geological Society of America, Washington, D. C., 1987.

Uyeda, S., and H. Kanamori, Back-arc opening and the mode of subduction, *J. Geophys. Res., 84*, 1049–1061, 1979.

Vogt, P.R., A. Lowrie, D. Bracey, and R.N. Hey, Subduction of oceanic ridges: Effects on shape, seismicity and other characteristics of consuming plate boundaries, *Spec. Pap. Geol. Soc. Am., 172*, 59 pp., 1976.

Welc, J.L., and T. Lay, The source rupture of the great Banda Sea earthquake of November 4, 1963, *Phys. Earth Planet. Inter., 45*, 242–254, 1987.

Wiens, D.A., Oceanic intraplate seismicity: Implications for the rheology and tectonics of the oceanic lithosphere, Ph.D. dissertation, 220 pp., Northwestern Univ., Evanston, Il., 1985.

Woodhouse, J.H., The excitation of long-period seismic waves by a source spanning a structural discontinuity, *Geophys. Res. Lett., 8*, 1129–1131, 1981.

P. R. Lundgren, Istituto Nazionale di Geofisica, Via di Villa Ricotti, 42, 00161 Rome, Italy.

E. A. Okal, Department of Geological Sciences, Northwestern University, Evanston, IL 60208.